International Journal of Reconfigurable and Embedded Systems (IJRES)
Vol. 15, No. 3, November 2026, pp. 693~704
ISSN: 2089-4864, DOI: 10.11591/ijres.v15.i3.pp693-704

Field-programmable gate array-based traffic detection unit using anisotropic magnetoresistive sensor

Sofiane Benzid[1,2], Ahmed Belhani[2,3]
[1]Department of Electronics, Faculty of Sciences and Technology, University Frères Mentouri Constantine 1, Constantine, Algeria
[2]Laboratory of Satellites, Artificial Intelligence, Cryptography, Internet of Things (LSIACIO), Department of Electronics, Faculty of Sciences and Technology, University Frères Mentouri Constantine 1, Constantine, Algeria
[3]Department of Process Engineering, Faculty of Process Engineering, University of Constantine 3, Constantine, Algeria

Article Info

Article history:

Received Feb 2, 2026
Revised Jul 9, 2026
Accepted Jul 18, 2026

Keywords:

Congestion
Field-programmable gate array
Intelligent transportation systems
Magnetic sensor
Sensor node
Traffic detection

ABSTRACT

The increasing impact of traffic congestion in urban areas has intensified research efforts toward the development of intelligent transportation systems (ITS) aimed at reducing congestion-related economic losses, improving commuter experience by minimizing travel delays, and mitigating environmental pollution caused by vehicular emissions. Wireless sensor networks (WSNs) have emerged as an effective solution for implementing ITS systems due to their low deployment cost, compact size, and flexible wireless communication capabilities. These networks are composed of multiple sensor nodes, which serve as the fundamental building blocks for acquiring real-time traffic information. In this paper, a traffic detection sensor node is developed on a field-programmable gate array (FPGA), exploiting its reconfigurable architecture to overcome the limited flexibility of conventional ASIC- and microcontroller-based solutions. The proposed design offers hardware adaptability, high processing capability, and scalability, making it suitable for evolving traffic monitoring requirements and future system extensions. Vehicle passage is detected using a magnetic sensor that captures changes in the earth's magnetic field resulting from vehicle movement, while wireless data transmission is achieved using the ZigBee communication protocol. Experimental results conducted under real urban traffic conditions demonstrate that the proposed system reliably detects and transmits vehicle magnetic signatures, achieving a detection accuracy of 93.2%.

This is an open access article under the CC BY-SA license.

Corresponding Author:

Sofiane Benzid
Department of Electronics, Faculty of Sciences and Technology, Frères Mentouri University-Constantine 1
325 Route de Ain El Bey, Constantine, Algeria
Email: sofiane.benzid@umc.edu.dz

1. INTRODUCTION

The majority of cities worldwide, particularly those with high population densities, are increasingly affected by traffic congestion due to the continuous growth in the number of vehicles outpacing the expansion of transport infrastructure [1]. The 2025 Urban Mobility Report published by the Texas A&M Transportation Institute highlights the severity of congestion in the United States [2]. For example, in 2024, congestion imposed an additional 9.8 billion hours of travel time on urban Americans, during which 10.6 billion liters of extra fuel were consumed, resulting in a total congestion cost of $269 billion, or approximately $1,480 per commuter. In Europe, congestion is similarly significant. According to the 2025 INRIX Traffic Scorecard [3], an average auto commuter in Istanbul lost 118 hours annually due to congestion, compared to 91 hours in London and 90 hours in Paris, reflecting the substantial economic and social burden of urban traffic delays.

One effective approach to mitigating the impact of traffic congestion is the development of intelligent transportation systems (ITS). ITS aim to improve the experience of commuters by reducing delays and the economic costs of congestion, enhancing safety, and providing real-time information on road conditions. These systems rely heavily on sensors to collect data related to traffic flow and road status [1]. A particularly efficient way to implement ITS is through wireless sensor networks (WSNs), which are composed of numerous low-cost, compact entities known as sensor nodes. Thanks to their wireless communication capabilities, these nodes can be easily deployed to collect traffic parameters such as vehicle count, speed, and type, as well as to detect accidents and emergency vehicles. Collected data can be leveraged by a traffic monitoring controller (TMC) to dynamically optimize traffic light plans at intersections, thereby alleviating congestion. A typical sensor node comprises sensing, processing, communication, and power supply units, enabling it to operate autonomously while contributing to the overall network.

Sensors play a central role in ITS by enabling real-time monitoring of traffic and, in some cases, environmental conditions that influence traffic flow. They are widely employed for vehicle counting, speed measurement, lane occupancy estimation, and vehicle classification, as well as for detecting traffic incidents and the presence of emergency vehicles. Various sensing technologies are employed to extract traffic parameters. For example, inductive loop detectors are used in [4] to measure multiple dynamic vehicle characteristics, including vehicle length, speed, wheelbase, and overhangs. Belenguer *et al.* [5] proposed integrating radio frequency identification (RFID) technology with existing inductive loop detectors installed on roadways to enable the extraction and exchange of information related to different vehicles. Vision-based systems are adopted in [6] for vehicle detection, speed estimation, and traffic flow counting. Infrared (IR) sensing has been applied for real-time vehicle and pedestrian detection under low-visibility conditions [7], as well as for traffic density estimation [8]. Ultrasonic sensors have been employed for vehicle detection and intersection traffic management [9], and for vehicle length and speed estimation [10].

As an alternative to the aforementioned traffic sensing technologies, anisotropic magnetoresistance (AMR) sensors are among the most widely adopted solutions in the literature for vehicle detection. These sensors operate by exploiting the near-uniform nature of the Earth's magnetic field and detecting its local disturbances caused by passing ferromagnetic objects such as vehicles. Compared with other traffic sensors, AMR sensors offer several advantages. They are mechanically robust and insensitive to vibrations, exhibit high sensitivity and long-term stability in capturing magnetic signatures under varying environmental and climatic conditions, and are compact and low-cost, which facilitates large-scale and dense deployment in ITS [11]. In addition, AMR sensors are easy to install, particularly when compared to inductive loop detectors that require pavement cutting and lane closure. They are also significantly less expensive than vision-based camera systems and are inherently immune to variations in weather conditions and daylight, unlike IR-based sensing technologies. Table 1 compares common traffic-detection technologies in terms of installation, performance, cost, and limitations.

Table 1. Comparison of traffic detection technologies

Technology	Installation	Performance	Cost/scalability	Limitations
Inductive loop detectors [4]	Intrusive; pavement cutting required	High accuracy	High installation/maintenance cost	Pavement damage; disruptive maintenance
RFID technology [5]	Roadside readers or embedded units	Reliable identification	Moderate cost; scalable with tag adoption	Requires tagged vehicles
Vision-based cameras [6]	Non-intrusive; poles, power	Rich traffic data; supports classification	High cost; limited scalability	Affected by lighting, weather
IR sensors [7], [8]	Roadside or overhead	Moderate accuracy	Moderate cost	Sensitive to temperature, sunlight
Ultrasonic Sensors [9], [10]	Short-range roadside, overhead, or embedded	Good for short range/low speed	Low cost; easy small-scale deployment	Limited range; affected by rain, fog, and noise
AMR magnetic sensors [11]	Non-intrusive; roadside or in-pavement	High sensitivity; weather-independent	Low cost, low power, and scalable	Magnetic interference

Several recent studies rely on AMR sensors installed under the pavement or directly on the road surface to capture vehicle-induced magnetic disturbances. For example, the work reported in [12] employs a single pavement-installed AMR sensor for vehicle detection and classification, while [13] proposes an embedded magnetic sensor array arranged across the traffic direction to estimate vehicle position. Although such configurations benefit from close proximity to passing vehicles and strong magnetic signal sensitivity, pavement-level installation remains a practical limitation, as installation and maintenance operations are disruptive to traffic flow and may reduce system scalability and long-term deployability. In addition, these

studies mainly emphasize sensing concepts and detection strategies, with limited discussion of complete sensor node hardware architectures.

Other contributions emphasize magnetic signal modeling and processing using commercially available triaxial magnetic sensors. Feng *et al*. [14], a triaxial RM3100 sensor is employed for vehicle detection, identification, and speed estimation through magnetic field disturbance modeling on a single lane, and the study suggests the use of an embedded sensing platform for data acquisition and processing. A similar signal-processing-oriented approach is presented in [15], where vehicle classification and speed interval estimation are performed using magnetic data acquired through a wired connection to an external computing unit, without wireless communication. Likewise, Zhang and Huang [16] investigates vehicle detection and classification using three-axis magnetic measurements combined with feature extraction and learning-based methods within a wireless sensor node architecture. While these works demonstrate the effectiveness of AMR-based sensing and advanced processing techniques, the primary focus remains on signal analysis and algorithm development rather than on the systematic design of modular and reconfigurable sensing platforms.

More integrated traffic monitoring solutions have been proposed through smart AMR-based sensing nodes that combine sensing, processing, and communication. The system described in [17] implements a battery-powered magnetic sensing node capable of vehicle counting and classification, with wireless data transmission to an access infrastructure. Similarly, the smart road stud (SRS) architecture presented in [18] integrates an AMR sensor, local processing, and short-range wireless communication to extract traffic parameters directly at the node level. Despite their higher level of system integration, these approaches still rely on road-surface or pavement-embedded installations, which may complicate large-scale deployment and routine maintenance in real traffic environments.

Several other studies have focused on enhancing detection robustness under challenging traffic conditions. Vehicle detection and classification using a single AMR sensor in highway scenarios are investigated in [19], with emphasis on detection logic and learning-based classification techniques. A triaxial AMR sensor embedded in lane markings is used to discriminate vehicle position and address simultaneous vehicle passages [20]. Roadside AMR-based vehicle classification is explored in [11], where feature extraction and time-series matching techniques are applied to distinguish common vehicle categories while minimizing interference with traffic flow. Multi-sensor configurations for speed and flow estimation are examined in [21], and adaptive detection strategies for congested traffic conditions are proposed in [22]. Although these works enhance detection robustness and functional scope, many still prioritize algorithmic improvements over the use of flexible and reconfigurable hardware platforms suitable for future ITS evolution.

In parallel with the evolution of WSNs, field-programmable gate array (FPGA)-based sensor nodes have attracted increasing attention in internet of things (IoT) and reconfigurable embedded-system research. Compared with conventional microcontroller-based platforms, modern FPGA devices provide hardware-level parallelism, high processing capability, and architectural reconfigurability, while also supporting computationally intensive tasks such as cryptography, data compression, and image processing [23]. Among recent contributions, the work in [24] proposed the FlexiS platform, a flexible FPGA-based sensor node capable of handling computation-intensive tasks such as feature extraction and local data processing. The same authors further extended this direction in [25] by introducing a reconfigurable wireless sensor-node architecture that supports remote FPGA reprogramming after deployment, thereby reinforcing the role of reconfigurability in IoT-oriented sensing systems. More recently, Leelakrishnan and Chakrapani [26] investigated a softcore-based FPGA architecture for WSNs with emphasis on power optimization, highlighting the potential of embedded processor logic inside the FPGA for improving node efficiency and reducing control overhead.

Other works have explored alternative FPGA-based processing strategies within WSNs. Bengherbia *et al.* [27] proposed a MicroBlaze-based WSN sink node using an XBee transceiver, illustrating the use of a vendor-specific softcore processor for communication and node control in FPGA-based sensor systems. In another contribution, an FPGA-based wireless sensor node with an embedded ADALINE neural-network coprocessor for vibration monitoring and fault diagnosis is presented in [28], demonstrating the suitability of FPGA platforms for implementing advanced signal-processing and intelligent algorithms directly at the sensor-node level.

Works addressing ITS through FPGA-based sensor node implementations remain limited in the literature. Existing contributions mainly focus on algorithm acceleration rather than complete FPGA-based sensing node design. For example, Wójcikowski *et al.* [29] presents an FPGA-based real-time implementation of a detection algorithm for traffic surveillance sensor networks, while [30] proposes an FPGA-based accelerator for vehicle detection and tracking. However, both works focus on processing functions and do not address full sensor node implementation, including sensing, communication, and embedded system integration. Similarly, the work reported in [31] proposes an FPGA-based smart traffic light controller integrating RFID and IR sensors to detect traffic conditions and dynamically adjust signal phases. However, the system was not validated under real outdoor conditions, and the sensing stage relied on switch-based emulation on the Altera

DE2 educational FPGA board rather than on physical sensor devices, which limits the assessment of its practical performance.

A closer analysis of the literature reveals that existing works can be divided into two main categories. The first includes application-specific traffic detection systems, which achieve strong sensing performance and real-world validation but rely on fixed microcontroller-based architectures with limited flexibility and scalability. The second includes FPGA-based IoT sensor nodes, which emphasize reconfigurability and edge processing, with limited focus on ITS applications, particularly those based on magnetic sensing technologies. Consequently, a clear gap exists between traffic-oriented sensing systems and reconfigurable IoT sensor-node architectures.

The proposed work addresses this gap by introducing a non-intrusive roadside AMR-based vehicle detection node built on a reconfigurable FPGA platform. Magnetic disturbances caused by passing vehicles are captured by the AMR sensor and processed locally on the FPGA using an adaptive thresholding algorithm based on the mean absolute deviation (MAD), which provides robust detection under varying noise levels and environmental conditions without requiring prior calibration. The resulting magnetic signatures are transmitted wirelessly via ZigBee to a receiving node, where additional filtering and event validation based on peak-to-peak signal amplitude are performed to suppress noise and reject interference from adjacent-lane vehicles. The proposed system was experimentally validated under real road conditions with different vehicle types and road configurations, achieving a detection accuracy of up to 93.2%.

Compared to conventional microcontroller-based solutions, the proposed design leverages an FPGA to enable high processing performance, real-time operation, and architectural reconfigurability. In addition, an open-source softcore processor is implemented on an Artix-7 FPGA, ensuring flexibility, vendor independence, and ease of customization for future ITS functionalities such as vehicle classification and speed estimation. This paper is organized as follows: section 2 describes the hardware and software implementation of the proposed traffic detection unit, section 3 presents the results and discussion of our implemented system, and section 4 concludes the paper.

2. DESIGN STRATEGY

Traffic detection is based on the principle that vehicles passage causes a distortion in the Earth's magnetic field. This distortion is sensed by a magnetic sensor which is in our case the 3-axes QMC5883 AMR sensor hosted on the GY-271 chip placed on the roadside, the magnetic signal is continuously transmitted to the processing unit built inside the Xilinx Artix-7 FPGA circuit hosted on the Xilinx Digilent Basys 3 board. When a vehicle passage is detected, the magnetic signature is transferred to a nearby PC, acting as a receiving node, using RF XBee modules. Figure 1 illustrates the block diagram of our designed sensor node for traffic detection, the components in dashed line are only needed during development process.

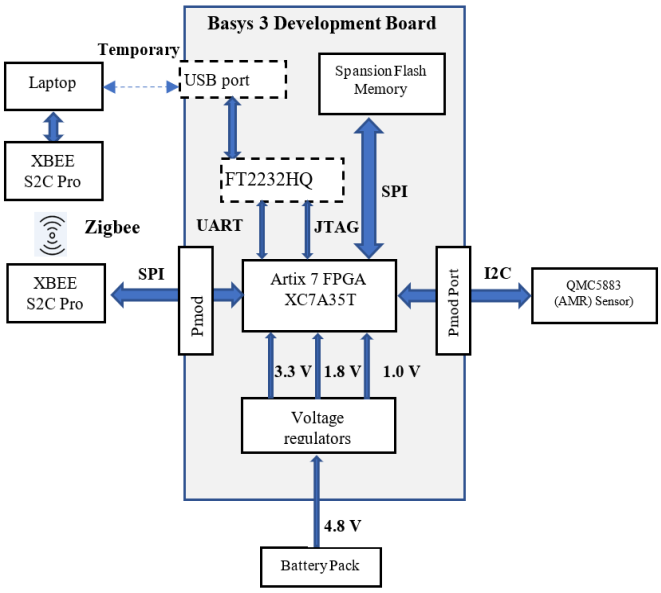


Figure 1. Sensor node design block diagram

2.1. Hardware design

In our sensor node, we distinguish two design parts: on-chip design which is the microcontroller system built on the FPGA circuit and constitutes a system-on-chip (SoC) and the off-chip design which represents the sensing unit, the wireless communication unit, the power unit, a flash memory, and voltage regulators. The communication between the microcontroller system unit and the sensing unit is based on I2C protocol whereas with communication unit is based on the SPI protocol.

2.1.1. On-chip design

The on-chip design corresponds to the microcontroller system synthesized and implemented on the FPGA circuit. Figure 2 represents the architecture of our sensor node showing the relationship between the microcontroller system and the other off-chip components. For the sake of clarity, auxiliary elements such as the flash memory and voltage regulation circuitry are omitted from the figure.

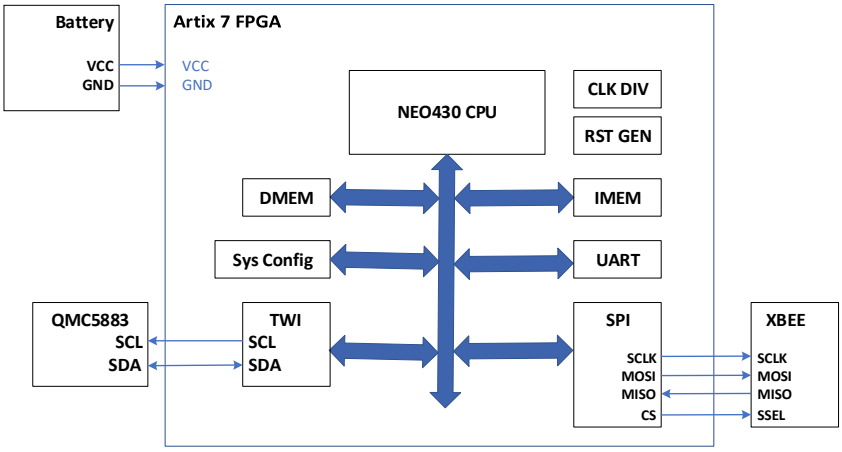


Figure 2. Sensor node architecture

The processing unit adopted in this work is an open-source, configurable soft microcontroller system known as NEO430 [32]. NEO430 is a very high speed integrated circuits hardware description language (VHDL)-described clone of the TI MSP430 microcontroller, built around the NEO430 16-bit RISC soft processor and supported by a set of ready-to-use, customizable peripheral modules. The Xilinx Vivado design suite is used to configure the VHDL project according to the requirements of the proposed design and to carry out the complete implementation flow, including synthesis, mapping, and bitstream generation. The resulting configuration is programmed onto the Artix-7 FPGA hosted on the Basys 3 board via the Digilent USB-JTAG interface and the FT2232HQ controller, as illustrated in the block diagram of Figure 1.

As mentioned earlier, the NEO430 system provides a set of optional peripheral modules that can be selectively included or removed during the synthesis process in order to optimize FPGA resource utilization. The peripheral modules relevant to this work are illustrated in Figure 2 and include the instruction memory (IMEM), data memory (DMEM), clock divider (CLK_DIV), universal asynchronous receiver-transmitter (UART), serial peripheral interface (SPI), and two wire interface (TWI) modules. IMEM provides 4 KB of instruction memory for application program storage and is configurable up to 48 KB, while DMEM offers 2 KB of data memory with a configurable capacity of up to 12 KB. The CLK_DIV module generates multiple clock frequencies required for the proper operation of communication peripherals such as UART, TWI, and SPI. The UART module is used as a communication interface for loading and testing application programs during the development phase. The SPI master module is employed to interface with the XBee wireless module using the SPI communication protocol; according to the XBee SPI specifications, it is configured to operate at a clock frequency of 1.5 MHz with 8-bit data, CPHA mode 0 (data sampled on the first clock edge), and most significant bit (MSB) transmitted first, with all settings applied through software by configuring the SPI control registers. In addition, the TWI module implements an I2C master interface used to communicate with the AMR sensor described later, with a software-configured clock frequency set to 100 kHz.

2.1.2. Off-chip design

The off-chip design comprises all circuitry external to the FPGA, including the sensing unit, wireless communication unit, flash memory, power supply, and voltage regulation stages. Vehicle detection is achieved

using a QMC5883 AMR sensor, which is a compact three-axis magnetic sensor integrating a 16-bit ADC. The sensor communicates with the FPGA-based processing unit via the I2C protocol, implemented through the TWI module of the NEO430 microcontroller system. It is mounted on a GY271 breakout board that provides the necessary pull-up resistors for reliable I2C operation. Magnetic field measurements are acquired by interfacing the sensor with the FPGA through a Pmod connector, which supplies power and digital signals and facilitates straightforward integration of external peripherals.

After a vehicle's magnetic signature is captured and processed, the resulting data are transmitted wirelessly to a nearby computer acting as the receiving node using the ZigBee protocol via a commercial XBee S2C Pro module. Communication between the FPGA and the XBee module is handled through the SPI interface using the NEO430 SPI peripheral. End-to-end wireless communication is enabled by employing two XBee modules configured using the XCTU software tool. The sensor-node-side module is connected to the FPGA through a Pmod interface and operates as an SPI slave, while the receiving module is connected to the PC via USB and communicates using the UART protocol. Both modules operate in ZigBee API mode 1, allowing data to be exchanged as structured serial packets to ensure reliable and organized wireless transmission.

By default, the final bitstream corresponding to the on-chip configuration is loaded into the SRAM-based configuration memory of the FPGA, which is volatile and requires reprogramming after each power cycle or reset. To enable non-volatile operation, the programming mode of the Basys 3 board is switched from USB-JTAG to flash-based configuration, using the onboard Spansion flash memory (Figure 1) to store the bitstream and automatically configure the FPGA at startup. The flash device interfaces with the FPGA through an SPI link and is programmed using the Vivado Design Suite. Power for the sensor node is provided by a rechargeable battery pack composed of four 1.2 V AA cells, delivering a nominal 4.8 V supply. Linear voltage regulators LTC3633+LTC3621 integrated on the Basys 3 board generate the regulated voltage levels required for stable FPGA operation, as illustrated in Figure 1. Figure 3 shows a real picture of our sensor node design; the flash memory and the voltage regulators are located on the back of the Basys 3 board.

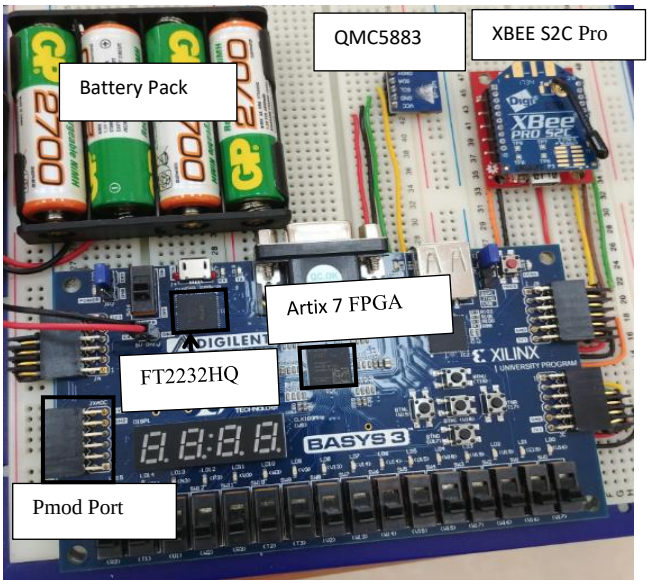


Figure 3. Sensor node components

2.2. Experimental set-up

In the experimental setup, the sensor node is installed on the roadside at an approximate distance of 1 m from the passing vehicles. As illustrated in Figure 4, the AMR sensor is oriented such that its Z-axis is perpendicular to the plane containing the moving vehicle, while the X-axis is aligned with the opposite direction of the traffic lane and the Y-axis is oriented vertically upward, perpendicular to the road surface. Experimental observations indicate that the Z-axis magnetic field component exhibits the highest sensitivity to vehicle-induced disturbances compared to the X and Y components; therefore, this component is used for vehicle detection in the proposed system.

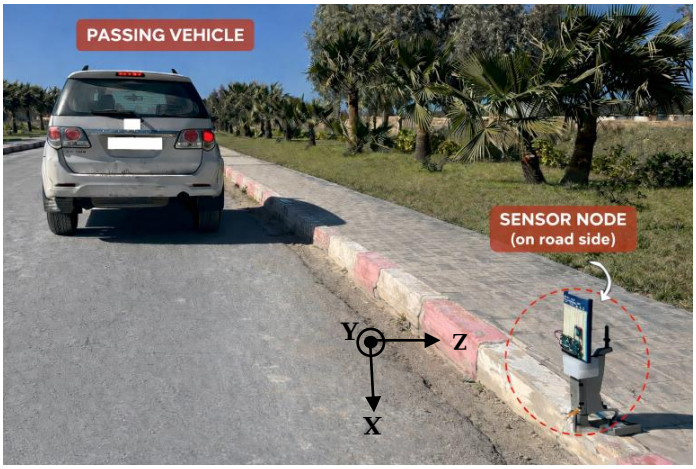


Figure 4. Experimental setup

2.3. Software design

This section outlines the software workflow used for vehicle detection and magnetic signature acquisition. The embedded C program running on the FPGA-based processing unit continuously samples the three-axis magnetic field from the AMR sensor and identifies vehicle passage events in real time. The detection algorithm is based on MAD adaptive thresholding, where a deviation measure is computed around the local mean of the signal. For a sliding window of N magnetic samples z_i, the baseline is first estimated as the mean value of the window using (1), which serves as a dynamic reference for subsequent analysis. Next, the MAD is calculated as shown in (2) and finally, the adaptive threshold T is given in (3):

$$\mu = \frac{1}{N}\sum_{i=1}^{N} z_i \tag{1}$$

$$MAD = \frac{1}{N}\sum_{i=1}^{N} |z_i - \mu| \tag{2}$$

$$T = K \cdot MAD \tag{3}$$

where K denotes a scaling factor that controls the trade-off between sensitivity and robustness. Larger values of K reduce false positives due to noise and adjacent-lane interference but may miss weak vehicle signatures, whereas smaller values increase detection sensitivity at the expense of higher false positive detection rates. In our design, K is tuned experimentally on-site. A vehicle event is declared whenever the deviation of the current sample from the local mean satisfies:

$$|z - \mu| > T \tag{4}$$

Upon detection, the corresponding magnetic signature is transmitted wirelessly in real time via ZigBee to a nearby PC acting as the receiving node, where a Python-based program first applies a moving average filter with a window size W=5 to smooth the incoming signal. The detection process is then further refined through a second-stage event validation based on the peak-to-peak amplitude of the filtered received signal. This additional verification step filters out false detections caused by noise or adjacent-lane interference, thereby improving system robustness while preserving real-time operation. For a detected event within a time window of M samples of filtered zf data, the peak-to-peak amplitude is defined as (5):

$$A_{pp} = \max(zf_i) - \min(zf_i), i = 1,2,\dots,M \tag{5}$$

An event is validated as a true vehicle detection if:

$$A_{pp} > T_{pp} \tag{6}$$

Where T_{pp} is a predefined validation threshold set experimentally.

The PC-side program also handles data storage, filtering, and visualization. The detection window is set to 1 s, during which 40 samples are acquired at 25 ms intervals. The main steps of the program are summarized in the flowchart shown in Figure 5.

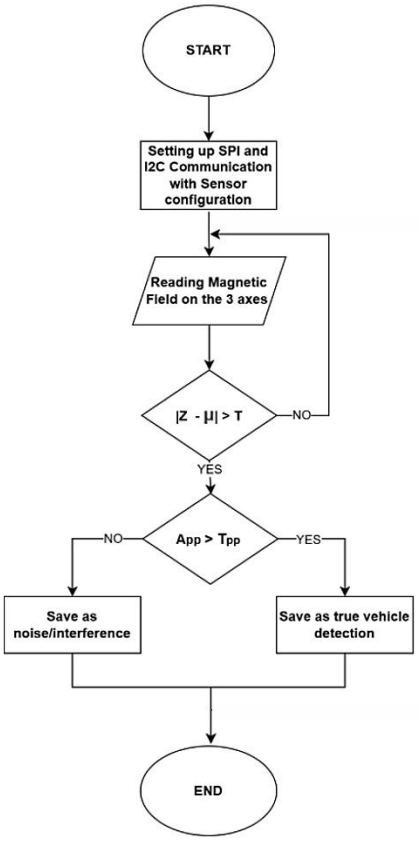


Figure 5. Vehicle detection flowchart

Initially, the I2C and SPI interfaces are configured, with the I2C clock set to 100 kHz for communication with the AMR sensor and the SPI clock set to 1.5 MHz for interfacing with the XBee module. The AMR sensor is then configured to operate at a 50 Hz output data rate, a ±2 G measurement range, and in continuous measurement mode. The program subsequently enters a continuous acquisition loop, where magnetic field measurements are read and vehicle passage is detected by monitoring the Z-axis component using MAD-adaptive thresholding algorithm. Following detection, the acquired magnetic data are then packaged into a ZigBee API mode 1 frame before being transmitted to the receiving XBee module connected to the PC. On the receiving side, the Python program extracts the magnetic samples, filters the signal and run the event validation based on the peak-to-peak amplitude. This validation stage discriminates true vehicle detection events from spurious responses caused by noise or adjacent-lane.

The open-source *TI msp430-gcc* compiler toolchain is used to generate a NEO430 executable from the application C/C++ source code in binary format (.bin). The resulting executable is then uploaded to the internal memory of the NEO430 microcontroller system as a VHDL memory image using the NEO430 bootloader. During the program development and debugging phases, communication between the host PC and the NEO430 system is established through the USB-UART interface implemented via the FT2232HQ controller on the Digilent Basys 3 board, with TeraTerm software employed as the serial terminal for program loading, monitoring, and interaction.

3. RESULTS AND DISCUSSION

3.1. On-chip system implementation result

Figure 6 shows RTL schematic of the implemented SoC system generated using Xilinx Vivado software showing the relationship between the different blocks of the NEO430 softcore microcontroller system

and the I/O signals of QMC5883 AMR sensor and the XBee module. In our design, a user pushbutton of Basys 3 board is used for system reset and 100 MHz as the main input clock.

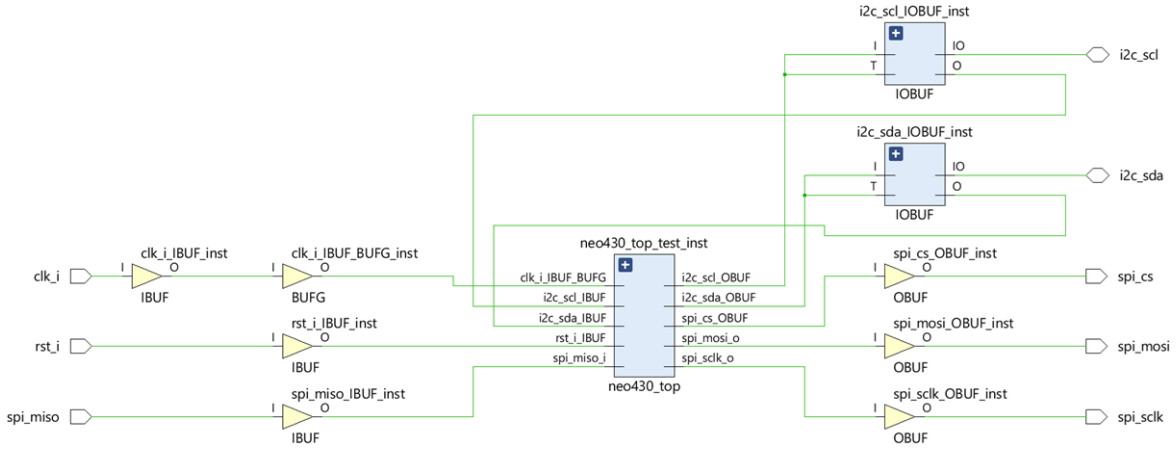


Figure 6. Schematic diagram of the on-chip system of the traffic detection unit

After synthesis and implementation, Vivado offers a summary of the FPGA resources used to implement our on-chip design along with power consumption of our system when the industrial version of Artix-7 is selected. Table 2 shows the utilization of the FPGA resources where the input/output (I/O) blocks are the most used resources with 8.49% while less than 5% are observed for the rest of the resources. The use of resources is very low which offers the possibility of expanding our design without extra physical circuitry relying on the flexibility and the programmability features of our FPGA circuit.

Table 2. FPGA resources utilization

Resources	Utilization	Available	Utilization %
LUT	543	20800	2.61
LUTRAM	16	9600	0.17
FF	264	41600	0.63
BRAM	2	50	4.00
I/O	9	106	8.49

For power consumption, Figure 7 summarizes the power consumed by each design part. The total on-chip power consumption is 71 mW, comprising 87% static power and 13% dynamic power. The results indicate that the overall power consumption is primarily dominated by static power, which is largely technology-dependent and influenced by the FPGA device selection. In contrast, the proposed VHDL implementation has been carefully optimized to minimize logic utilization by retaining only the essential functional components, resulting in a low dynamic power consumption of approximately 9 mW.

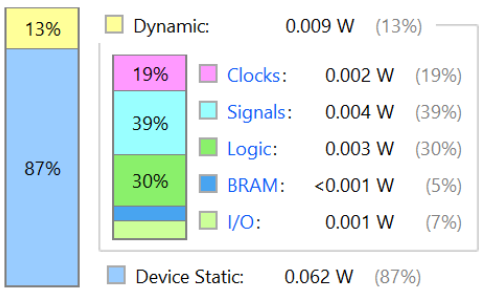
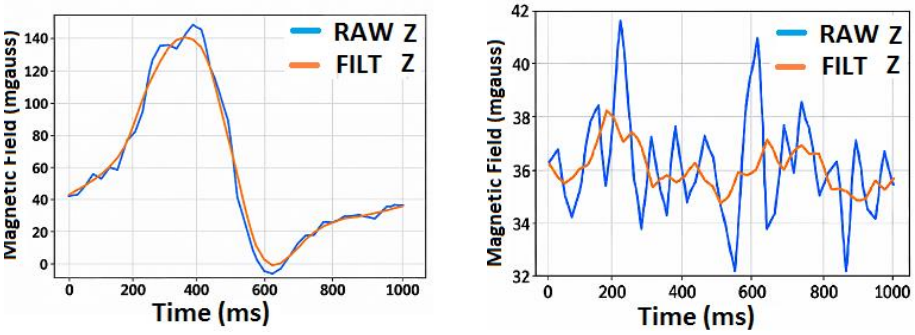


Figure 7. On-chip power consumption

3.2. Vehicle detection results

Experimental tests were conducted on different urban roads and vehicle types to evaluate the robustness of the proposed sensing unit for detecting magnetic signatures of passing vehicles. The system was deployed on a single-lane road side with a sensor distance of less than 1 m from the traffic lane and vehicle speeds ranging from 30 to 60 km/h. Figure 8 show two types of magnetic signals, Figure 8(a) which corresponds to a valid vehicle magnetic signature, while Figure 8(b) illustrates a rejected noise signal.



(a) (b)

Figure 8. Magnetic signatures of: (a) valid car passage and (b) rejected noise signal

Detection results are summarized in Table 3; a total of 111 vehicle passages were recorded. Among them, 109 were correctly detected, while 4 false positive detections were observed due to noise and electromagnetic interference of adjacent lane. In addition, 2 false negative detections occurred when weak magnetic signal vehicles were incorrectly classified as noise. These results correspond to an overall detection accuracy of 93.2%, confirming the effectiveness of the proposed approach under real traffic conditions.

Table 3. Traffic detection results

Detection events	Observed vehicles	Detected vehicles	Flase positives	False negatives	Accuracy (%)
117	111	109	04	02	93.2

These results demonstrate the effectiveness of the proposed sensor node in reliably detecting passing vehicles in a non-disruptive roadside deployment. Furthermore, extended analysis of magnetic signatures collected from a larger dataset of vehicles combined with the high performance, multiprocessing, and reconfigurability features of FPGA circuit, may enable the extraction of additional traffic-related parameters, such as vehicle type, length, and speed, thereby supporting more advanced ITS functionalities and contributing to improved traffic management and congestion mitigation.

4. CONCLUSION

This paper presented the design and implementation of a roadside traffic detection unit deployed in a non-disruptive manner. Vehicle passage is detected using an anisotropic magnetoresistive (AMR) sensor and an adaptive threshold algorithm, which captures the corresponding magnetic signatures, while processing is performed using an open-source softcore microcontroller implemented on an Artix-7 FPGA, with real-time wireless data transmission achieved via the ZigBee protocol. The proposed system effectively links magnetic sensing for ITS applications with the reconfigurability and flexibility of FPGA-based platforms. Furthermore, the use of an open-source softcore processor provides vendor independence and facilitates scalability, portability, and ease of modification across commercial off-the-shelf FPGA devices. Experimental results demonstrate the effectiveness of the proposed design, achieving a detection accuracy of 93.2% under real traffic conditions.

Despite these promising results, certain limitations were identified. The system exhibits reduced reliability in detecting slow-moving or stationary vehicles, which may lead to multiple detections of the same vehicle or missed detections in congested traffic scenarios. Additionally, vehicles traveling in adjacent lanes are more difficult to detect due to the increased distance from the sensor. Future work will focus on improving

detection robustness in dense and low-speed traffic conditions, as well as enhancing spatial selectivity to mitigate adjacent lane interference. Further developments will also explore the extraction of additional traffic parameters, such as vehicle speed and classification, from the recorded magnetic signatures.

FUNDING INFORMATION

Authors state no funding involved.

AUTHOR CONTRIBUTIONS STATEMENT

This journal uses the Contributor Roles Taxonomy (CRediT) to recognize individual author contributions, reduce authorship disputes, and facilitate collaboration.

Name of Author	C	M	So	Va	Fo	I	R	D	O	E	Vi	Su	P	Fu
Sofiane Benzid	✓	✓	✓	✓	✓	✓			✓				✓	
Ahmed Belhani	✓	✓		✓	✓	✓				✓	✓	✓		

C : **C**onceptualization
M : **M**ethodology
So : **So**ftware
Va : **Va**lidation
Fo : **Fo**rmal analysis
I : **I**nvestigation
R : **R**esources
D : **D**ata Curation
O : Writing - **O**riginal Draft
E : Writing - Review & **E**diting
Vi : **Vi**sualization
Su : **Su**pervision
P : **P**roject administration
Fu : **Fu**nding acquisition

CONFLICT OF INTEREST STATEMENT

Authors state no conflict of interest.

DATA AVAILABILITY

Derived data supporting the findings of this study are available from the corresponding author [initials, SB] on request.

REFERENCES

[1] S. Benzid and A. Belhani, "A Study of Wireless Sensor Networks Based Adaptive Traffic Lights Control," in *Lecture Notes in Networks and Systems*, vol. 413, pp. 406–417, 2022, doi: 10.1007/978-3-030-96311-8_37.
[2] D. Schrank, L. Albert, K. Jha, and B. Eisele, *2025 Urban Mobility Report*. College Station, TX, USA: Texas A&M Transportation Institute, 2025.
[3] B. Pishue, *2025 INRIX Global Traffic Scorecard*. Bellevue, WA, USA: INRIX, Dec. 2025.
[4] Z. Marszalek and K. Duda, "Validation of Multi-Frequency Inductive-Loop Measurement System for Parameters of Moving Vehicle Based on Laboratory Model," *Sensors*, vol. 24, no. 22, pp. 1–19, Nov. 2024, doi: 10.3390/s24227244.
[5] F. M. Belenguer, A. Martínez-Millana, A. M. Salcedo, and J. H. A. Núñez, "Vehicle Identification by Means of Radio-Frequency-Identification Cards and Magnetic Loops," *IEEE Transactions on Intelligent Transportation Systems*, vol. 21, no. 12, pp. 5051–5059, Dec. 2020, doi: 10.1109/TITS.2019.2948221.
[6] A. R. Vyas and P. J. Patel, "Real-Time Traffic Surveillance and Vehicle Speed Detection Using Machine Vision," *Journal of Information Systems Engineering and Management*, vol. 10, no. 42s, pp. 313–326, 2025, doi: 10.52783/jisem.v10i42s.7890.
[7] X. Luo, H. Zhu, and Z. Zhang, "IR-YOLO: Real-Time Infrared Vehicle and Pedestrian Detection," *Computers, Materials and Continua*, vol. 78, no. 2, pp. 2667–2687, 2024, doi: 10.32604/cmc.2024.047988.
[8] Z. Talib and L. A. A. Rahaim, "Smart Traffic System Using Infrared Sensors-based IoT," *Journal of Internet Services and Information Security*, vol. 14, no. 3, pp. 29–41, Aug. 2024, doi: 10.58346/JISIS.2024.I3.003.
[9] M. Chauhan, R. Astya, S. Arora, and M. Gupta, "Real-time traffic management system based on ultrasonic sensors using LTE communication," *Journal of Integrated Science and Technology*, vol. 13, no. 8, p. 1181, Oct. 2025, doi: 10.62110/sciencein.jist.2025.v13.1181.
[10] J. L. Poza-Lujan, P. Uribe-Chavert, and J. L. Posadas-Yagüe, "Low-cost modular devices for on-road vehicle detection and characterisation," *Design Automation for Embedded Systems*, vol. 27, no. 1–2, pp. 85–102, Jun. 2023, doi: 10.1007/s10617-023-09270-y.
[11] X. Chen, X. Kong, M. Xu, K. Sandrasegaran, and J. Zheng, "Road Vehicle Detection and Classification Using Magnetic Field Measurement," *IEEE Access*, vol. 7, pp. 52622–52633, 2019, doi: 10.1109/ACCESS.2019.2908006.
[12] P. Sarcevic, S. Pletl, and A. Odry, "Real-Time Vehicle Classification System Using a Single Magnetometer," *Sensors*, vol. 22, no. 23, pp. 1–19, Nov. 2022, doi: 10.3390/s22239299.
[13] J. Balamutas *et al.*, "Passing Vehicle Road Occupancy Detection Using the Magnetic Sensor Array," *IEEE Access*, vol. 11, pp. 50984–50993, 2023, doi: 10.1109/ACCESS.2023.3278986.
[14] Y. Feng *et al.*, "MagMonitor: Vehicle Speed Estimation and Vehicle Classification Through A Magnetic Sensor," *IEEE Transactions on Intelligent Transportation Systems*, vol. 23, no. 2, pp. 1311–1322, Feb. 2022, doi: 10.1109/TITS.2020.3024652.
[15] W. Li, Z. Liu, Y. Hui, L. Yang, R. Chen, and X. Xiao, "Vehicle Classification and Speed Estimation Based on a Single Magnetic Sensor," *IEEE Access*, vol. 8, pp. 126814–126824, 2020, doi: 10.1109/ACCESS.2020.3008483.

[16] X. Zhang and H. Huang, "Vehicle Classification Based on Feature Selection with Anisotropic Magnetoresistive Sensor," *IEEE Sensors Journal*, vol. 19, no. 21, pp. 9976–9982, Nov. 2019, doi: 10.1109/JSEN.2019.2928828.
[17] W. Balid, H. Tafish, and H. H. Refai, "Intelligent Vehicle Counting and Classification Sensor for Real-Time Traffic Surveillance," *IEEE Transactions on Intelligent Transportation Systems*, vol. 19, no. 6, pp. 1784–1794, Jun. 2018, doi: 10.1109/TITS.2017.2741507.
[18] H. Wang, Y. Sun, W. Quan, X. Ma, and W. Y. Ochieng, "Traffic volume measurement based on a single smart road stud," *Measurement: Journal of the International Measurement Confederation*, vol. 187, p. 110150, Jan. 2022, doi: 10.1016/j.measurement.2021.110150.
[19] H. Dong, X. Wang, C. Zhang, R. He, L. Jia, and Y. Qin, "Improved Robust Vehicle Detection and Identification Based on Single Magnetic Sensor," *IEEE Access*, vol. 6, pp. 5247–5255, 2018, doi: 10.1109/ACCESS.2018.2791446.
[20] M. Liu, W. Hua, and Q. Wei, "Vehicle detection using three-Axis AMR sensors deployed along travel lane markings," *IET Intelligent Transport Systems*, vol. 11, no. 9, pp. 581–587, Nov. 2017, doi: 10.1049/iet-its.2017.0100.
[21] B. Santoso, B. Yang, C. L. Ong, and Z. Yuan, "Traffic flow and vehicle speed measurements using Anisotropic Magnetoresistive (AMR) sensors," in *2018 IEEE International Magnetics Conference (INTERMAG)*, IEEE, Apr. 2018, pp. 1–4, doi: 10.1109/INTMAG.2018.8508869.
[22] X. Bao, H. Li, D. Xu, L. Jia, B. Ran, and J. Rong, "Traffic vehicle counting in jam flow conditions using low-cost and energy-efficient wireless magnetic sensors," *Sensors*, vol. 16, no. 11, pp. 1–16, Nov. 2016, doi: 10.3390/s16111868.
[23] A. de la Piedra, A. Braeken, and A. Touhafi, "Sensor systems based on FPGAs and their applications: A survey," *Sensors*, vol. 12, no. 9, pp. 12235–12264, Sep. 2012, doi: 10.3390/s120912235.
[24] D. M. Pham and S. M. Aziz, "Flexis—a flexible sensor node platform for the internet of things," *Sensors*, vol. 21, no. 15, pp. 1–20, Jul. 2021, doi: 10.3390/s21155154.
[25] S. M. Aziz, D. H. Hoskin, D. M. Pham, and J. Kamruzzaman, "Remote reconfiguration of FPGA-based wireless sensor nodes for flexible Internet of Things," *Computers and Electrical Engineering*, vol. 100, pp. 1–14, May 2022, doi: 10.1016/j.compeleceng.2022.107935.
[26] S. Leelakrishnan and A. Chakrapani, "Power Optimization in Wireless Sensor Network Using VLSI Technique on FPGA Platform," *Neural Processing Letters*, vol. 56, no. 2, pp. 1–22, Mar. 2024, doi: 10.1007/s11063-024-11495-2.
[27] B. Bengherbia, S. Chadli, M. O. Zmirli, and A. Toubal, "A MicroBlaze based WSN sink node using XBee transceiver," in *2016 8th International Conference on Modelling, Identification and Control (ICMIC)*, IEEE, Nov. 2017, pp. 831–834, doi: 10.1109/ICMIC.2016.7804229.
[28] B. Bengherbia, R. Kara, A. Toubal, M. O. Zmirli, S. Chadli, and P. Wira, "FPGA implementation of a wireless sensor node with a built-in ADALINE neural network coprocessor for vibration analysis and fault diagnosis in machine condition monitoring," *Measurement: Journal of the International Measurement Confederation*, vol. 163, p. 107960, Oct. 2020, doi: 10.1016/j.measurement.2020.107960.
[29] M. Wójcikowski, R. Żaglewski, and B. Pankiewicz, "FPGA-based real-time implementation of detection algorithm for automatic traffic surveillance sensor network," *Journal of Signal Processing Systems*, vol. 68, no. 1, pp. 1–18, Jul. 2012, doi: 10.1007/s11265-010-0569-3.
[30] J. Zhai, B. Li, S. Lv, and Q. Zhou, "FPGA-Based Vehicle Detection and Tracking Accelerator," *Sensors*, vol. 23, no. 4, pp. 1–26, Feb. 2023, doi: 10.3390/s23042208.
[31] N. S. M. Hadis *et al.*, "Design and implementation of smart traffic light controller with emergency vehicle detection on FPGA," *International Journal of Reconfigurable and Embedded Systems*, vol. 14, no. 1, pp. 48–59, Mar. 2025, doi: 10.11591/ijres.v14.i1.pp48-59.
[32] S. Nolting, "NEO430.pdf." github.com, [Online]. Available: https://github.com/stnolting/neo430/blob/master/doc/NEO430.pdf. (Accessed: Mar. 10, 2025).

BIOGRAPHIES OF AUTHORS



Sofiane Benzid received his B.Sc. degree in Control Engineering from the Institute of Electrical and Electronics Engineering, University of Boumerdes, Boumerdes, Algeria, in 2013, and the M.Sc. degree in Embedded Systems from the National Higher School of Technology, Algiers, Algeria, in 2017. He is currently pursuing the Ph.D. degree in Embedded Systems at the University Frères Mentouri Constantine 1, Constantine, Algeria. His research interests include embedded and system-on-chip design, wireless sensor networks, and FPGA-based system implementations. He can be contacted at email: sofiane.benzid@umc.edu.dz.



Ahmed Belhani received his B.Sc. degree, master's degree and Ph.D. degree, all from Constantine 1 University, Algeria in 1995, 2000, and 2007, respectively. He is the head of research team "Automatics and Intelligent System" at the LSIACIO Laboratory in 2017. His works on nonlinear systems, intelligent systems, and embedded systems. He can be contacted at email: ahmed.belhani@univ-constantine3.dz.